# EXPERIMENTAL ANALYSIS OF BEAM-TO-COLUMN JOINTS EQUIPPED WITH SPRAYED ALUMINIUM FRICTION DAMPERS

Massimo Latour[a*], Vincenzo Piluso[a], Gianvittorio Rizzano[a]

[a]University of Salerno, Dept. of Civil Engineering, Italy
mlatour@unisa.it, v.piluso@unisa.it, g.rizzano@unisa.it

## ABSTRACT

In this paper, the results of an experimental analysis regarding beam-to-column joints equipped with friction dampers is presented. Even though the overall concept is not new, the connection structural detail and the friction pad material are different from previous proposals. In particular, the beam is connected to the column with a classical fixed T-stub fastening the upper flange and a friction damper located at the beam lower flange. The friction damper is composed of a stack of steel plates conceived to assure symmetrical friction. The friction pads are made of steel plates coated with thermally sprayed aluminium. The friction damper is designed in order to slide for a force level equal to or lower than the ratio between the nominal flexural resistance of the connected beam and the lever arm, i.e. the distance between the top T-stub and the friction damper. In this way, it is possible to obtain connections able to dissipate the seismic input energy almost without any damage to the steel elements, provided that all the joint components are designed with sufficient over-strength with respect to the actions corresponding to the friction damper sliding force. In this paper, such approach is validated reporting the results of an experimental campaign.

*Keywords: Friction dampers, Connections, Free from yielding, Sprayed Aluminum*

** Corresponding author*

## 1. INTRODUCTION

The design of modern seismic resistant structures is based on a preliminary selection of the zones which have to be designed to assure the dissipation of the earthquake input energy. Dealing with Moment Resisting Frames (MRFs), the location of such dissipative zones at the beam ends is commonly preferred by adopting full-strength beam-to-column joints [1,2] which have to be designed with sufficient over-strength with respect to the connected beams. The required over-strength is aimed to assure the beam end yielding despite of the influence of random material variability [3,4] and the amount of strain-hardening occurring before the complete development of the ultimate flexural resistance of plastic hinges [5,6].

To date, the classical design philosophy based on weak beam-strong column-strong joint hierarchy has been widely applied in practical seismic design and surely provides some advantages, such as the development of stable hysteresis loops [7-10] and the prevention of soft-storey mechanisms which have to be avoided because of their poor energy dissipation capacity [11]. However, some drawbacks occur within the framework of the traditional design approach. On one hand, the use of full-strength beam-to-column joints with the code required over-strength can lead to the detailing of expensive structural connections which require the use of continuity plates, supplementary column web plates, reinforcing ribs or cover plates or, even, the use of haunched beams. On the other hand, also the overall frame design is costly, because of the column over-strength required to fulfil the strength hierarchy criteria, particularly in the case of long span beams, whose size is governed by gravity loads [12-15].

In order to overcome the drawbacks related to the use of full-strength beam-to-column joints, the use of partial-strength connections has been suggested and Eurocode 8 [1] has opened the door to their use provided that their plastic rotation capacity is properly demonstrated. Such design approach can be faced within the framework of the component approach [15-18]. The fastening elements of the beam-to-column joints have to be properly designed by selecting the weakest joint component, acting as dissipative component, and providing all the other joint components with sufficient over-strength. Moreover, the weakest joint component has to be designed to assure a ductile behaviour and the required plastic deformation capacity [19].

In last decades the application of partial strength joints to MRFs has been proposed and supported by a high number of research programs, both theoretical and experimental, devoted to characterise the behaviour of connections under monotonic [20-22] and cyclic loading conditions [23-27]. Nevertheless, even though the effort provided by the scientific community has been significant, there are still some issues which deserve further investigation, such as the codification of design criteria for dissipative joints or the development of new types of dissipative connections easy to replace or not requiring replacement after a severe seismic event [28-31].

However, independently of the use of either full-strength or partial-strength beam-to-column joints, the main drawback of the traditional seismic resistant design strategy is intrinsic in the strategy itself. In fact, on one hand the structural damage is essential to dissipate the earthquake input energy but, on the other hand, it is the main source of direct and indirect losses. For this reason, many researchers have focused their attention on the strategy of supplementary energy dissipation with the aim to reduce the structural damage under destructive seismic events and, as a consequence, the direct and indirect losses. This strategy is based on the use of energy dissipation devices which have to be inserted between couples of points of the structural scheme where high relative displacements or velocities occur under the action of severe ground motions [33-36]. Such displacements or velocities are expected to activate specifically designed passive energy dissipation systems based on simple mechanisms such as hysteresis, friction or viscosity of fluids.

Starting from the background briefly summarized above, in order to overcome the drawback of the traditional design approaches, research efforts have been recently devoted to the practical development of a new design strategy whose goal is the design of connections able to withstand almost without any damage not only frequent and occasional seismic events, but also destructive earthquakes such as those corresponding to rare and very rare events.

The concept behind this research is inspired to the strategy of supplementary energy dissipation, but it is based on the use of damping devices under a new perspective. In fact, while passive control strategies have been commonly based on the integration of the energy dissipation capacity of the primary structure by means of a supplementary dissipation coming from damping devices; conversely, the new design strategy is based on the use of friction dampers conceived in such a way to substitute the traditional dissipative zones of MRFs, i.e. the beam ends. To this scope, beam-to-column connections can be equipped with friction dampers which can be located either at the level of the two flanges [37-39] or at the bottom flange level only [40-42]. Also the beam web to column flange connection can be equipped with friction dampers. Moreover, symmetrical [39, 43] or asymmetrical friction devices can be exploited [35, 38].

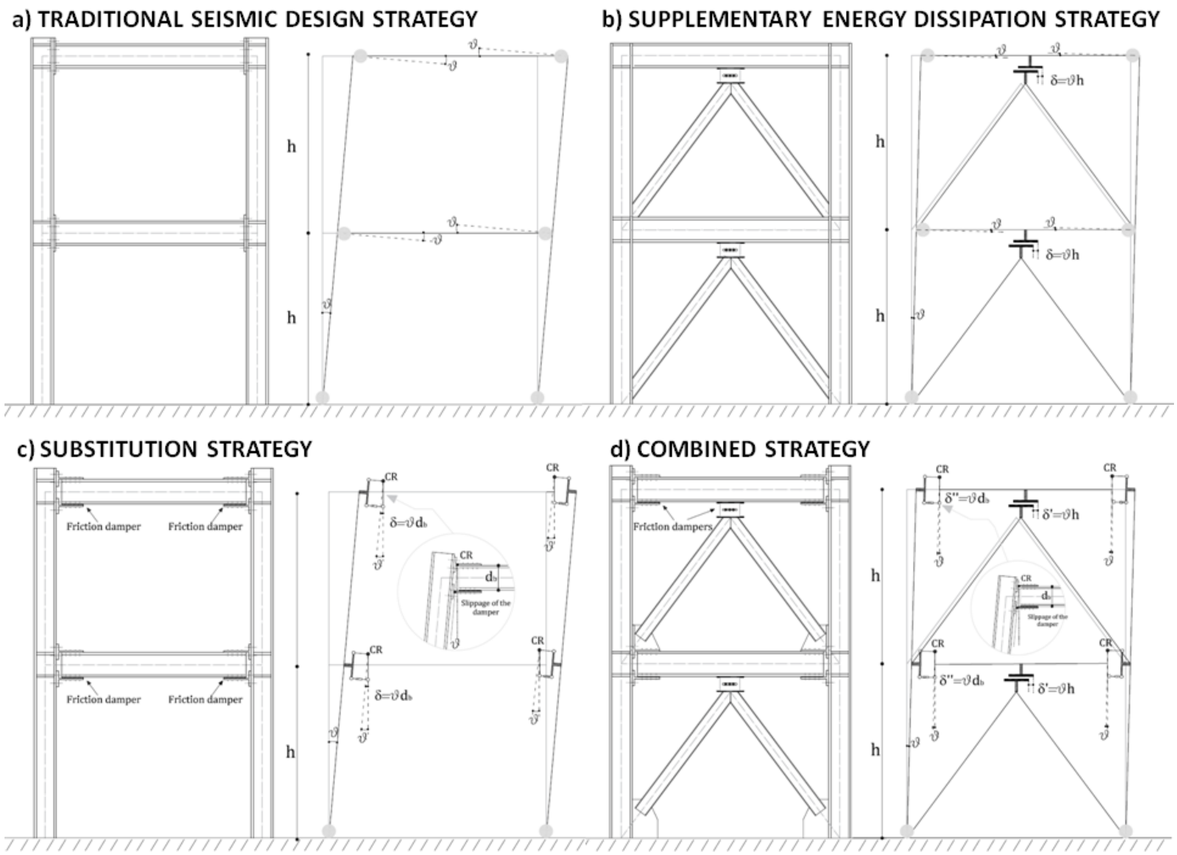


***Figure 1:*** *Comparison between different design strategies*

In order to well clarify the aim of the work, its framework and the differences with either traditional seismic design or supplementary energy dissipation strategy, the different schemes are analysed in Fig. 1. In particular, Fig. 1a points out that dissipative zones of traditional MRFs are located at the beam ends where plastic hinges have to be developed. The seismic demand is usually expressed in terms of maximum interstorey drift ($\vartheta$ in the figure) which governs the plastic rotation expected in dissipative zones. The supplementary energy dissipation strategy (Fig. 1b) is aimed to the reduction of the seismic demand by introducing seismic dampers which have to be located, for their effectiveness, between couple of points subjected to high relative displacements. The supplementary energy dissipation provided by such devices allows the reduction of the drift $\vartheta$ and, as a consequence, the reduction of the structural damage occurring at the beam ends. Conversely, the substitution strategy (Fig. 1c) allows the prevention of the structural damage, because all the dissipative zones are substituted by means of connections equipped with friction dampers. The expected drift demand does not reduce when comparison is made with traditional structures (Fig. 1a), but this drift leads to very limited structural damage in some joints components, because the rotation of the beam-to-column connections is accommodated by properly calibrating the stroke of the friction dampers (Fig. 1c). The maximum rotation allowed is practically given by the ratio between the damper stroke and the lever arm, i.e. its distance from the centre of rotation CR. However, it is useful to note that the relative displacement occurring between the ends of the friction damper ($\delta = \vartheta d_b$, being $d_b$ the beam depth) is significantly less than the one ($\delta = \vartheta h$, being $h$ the interstorey height) occurring when the supplementary energy dissipation strategy is applied (Fig. 1b). This is the main reason why cases a) and c) are expected to provide similar drift demands. Finally, the best solution is obtained by combining the substitution strategy with the supplementary energy dissipation strategy. Such combined strategy (Fig. 1d) leads both to the reduction of the drift demands expected in case of destructive seismic events and, in addition, to the prevention of significant damage in beam-to-column connections. Obviously, the drift reduction is also an important benefit to reduce damage to the building non-structural components.

Within the above framework, i.e. either substitution strategy or combined strategy, in this paper a new beam-to-column connection equipped with friction dampers is investigated. In particular, it is suggested to modify the classical detail of Double Split Tee Joints (DST) by introducing a symmetrical friction damper at the level of the lower beam flange. With the proposed connecting system, under bending actions, the joint is forced to rotate around the upper T-stub, preventing slab damage, and the energy dissipation supply is provided by the slippage of the lower beam flange on the friction pads which are made of steel plates coated with thermally sprayed aluminium. In this way, provided that the steel components of the connection are properly over-strengthened, the joint resistance and the rotation capacity can be easily governed by calibrating the preload applied to the frictional interfaces and realizing slotted holes whose length provides an adequate stroke for the dissipative device.

As the overall concept of equipping beam-to-column connections with friction dampers is not new, it is important to underline the main differences with respect to similar connections proposed by the New Zealand research group [39, 42, 44-45]. In particular, the main differences regard the type of friction damper adopted and the material used for the friction pads. In fact, the connection structural detail herein presented is based on the use of symmetric friction damper while the sliding hinge joint proposed by Clifton et al. is based on an asymmetric friction damper [39, 42]. The use of asymmetric friction dampers gives rise to some yielding of the bolts which are subjected to bending moment, shear and axial force. Such yielding is prevented when symmetric friction dampers are used like in the case of the beam-to-column connections herein experimentally investigated. Moreover, the friction pads of the connections herein investigated are made of steel plates coated by thermally sprayed aluminium; conversely, other researchers have adopted brass or steel [38], bisalloy steel grade [39, 42, 44-45] or brake lining pads [37].

In order to validate the proposed beam-to-column connection system, an experimental program has been carried out at the Materials and Structures Laboratory of Salerno University and the results obtained are herein presented. In particular, the results of preliminary tests aimed at characterizing the frictional properties of new pads coated by thermally sprayed aluminium are described and, afterwards, the results of two tests on real-scale external beam-to-column joints are presented. Furthermore, on the basis of the component method, a design procedure -has been developed and adopted to design the specimens The aim of the design procedure is to concentrate the energy dissipation in the friction damper and to prevent the yielding of all the other joint components.

## 2. EXPERIMENTAL ANALYSIS ON THERMALLY SPRAYED ALUMINUM INTERFACES

The results here presented constitute the further development of work already carried out in a previous experimental project dealing with the characterisation of frictional interfaces made of brass, steel and three different types of rubber [46, 47]. The results herein presented are referred to a new type of friction pad composed by an 8 mm S275JR steel plate (steel hardness 211 HBW, sand blasted surface) coated with a thermally sprayed thin layer of aluminium (Fig. 2). The use of thermally sprayed aluminium coatings can lead to high value of the friction coefficient [49], thus allowing the reduction of the size of the friction damper.

Even though not exhaustively, thermal spray can be defined as the application of coatings by means of special devices/systems through which melted or molten spray material is propelled at high speed onto a cleaned and prepared surface of the component to be coated. The coating feedstock material is melted by a heat source. This liquid or molten material is then propelled by process gases and sprayed onto a base material, where it solidifies and forms a solid layer.

There are several different processes to apply a thermal sprayed coating. The process applied for the friction pads herein investigated is the electric arc wire spray. Even though the main field of application of sprayed aluminium is the prevention of corrosion phenomena, the high values of the friction coefficient obtained and the low cost of the raw material have already suggested its use for friction pads in damping technology [48, 49].

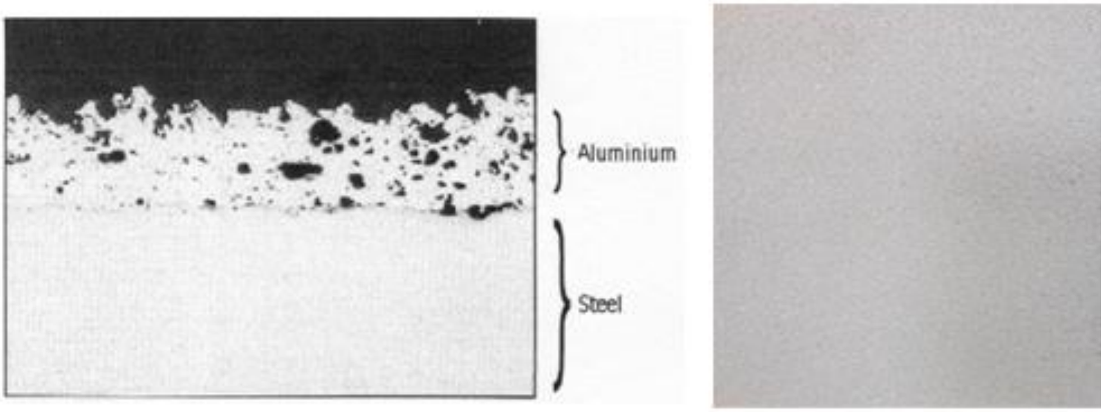


*a) Cross section of the coating* *b) Plan view of the surface*

***Figure 2:*** *Cross-section of the coating and texture of the tested materials*

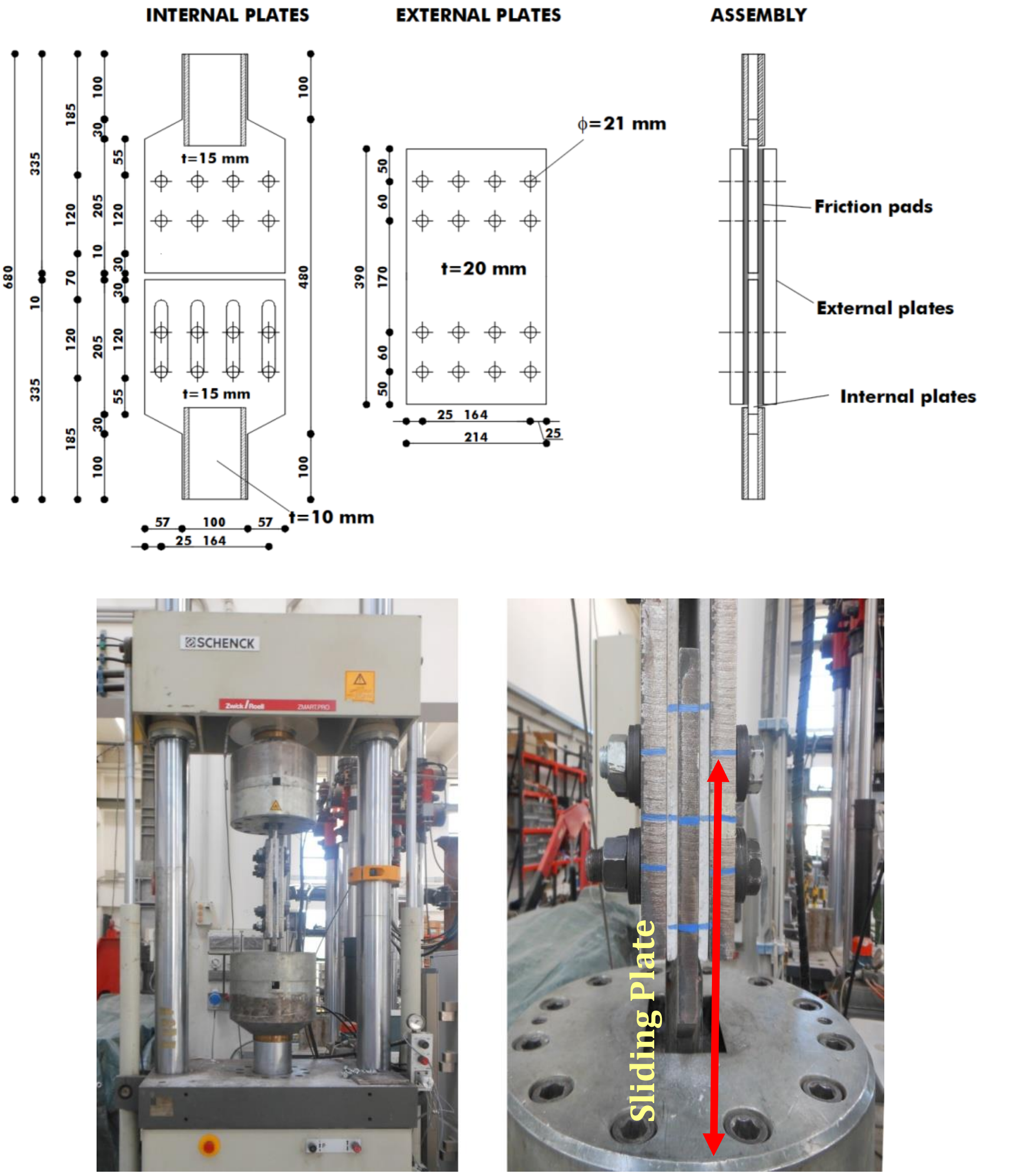


***Figure 3:*** *Geometry of specimens and testing equipment*

In order to evaluate the friction coefficient of interfaces made of steel plates sliding on thermally sprayed aluminium such as those adopted in the design of the proposed joint, a sub-assemblage composed by a stack of S275JR steel plates has been employed. The device has been designed to allow the slippage of one of the inner steel plates on the interposed material. To this scope, such plate is realised with slotted holes, while the other inner and the two outer plates are realised with circular holes (Fig. 3). The clamping force is applied to the friction pad by means of a maximum number of 8 high strength pre-loadable M20 bolts of 10.9 class [16, 50,51] and, in order to reduce preloading losses during the test, cone annular disc springs have been used in substitution of the classical circular flat washers [46, 47]. The disc springs adopted conform to standard DIN 6796. The tests have been carried out by means of a universal testing machine Schenck Hydropuls S56 (Fig. 3). In order to measure the axial displacements the testing device is equipped with an LVDT, while the tension/compression loads are measured by means of a load cell. The cyclic tests have been carried out under displacement control for different amplitudes at a frequency equal to 0.25 Hz. This value has been selected to be compatible with the capabilities of the testing equipment. Even though this frequency does not correspond to the values occurring under actual seismic events, it seems from the available technical literature that the influence of the velocity is not particularly significant. In fact, the sliding force versus velocity relationship can be modelled by means of a power expression where the exponent is close to zero [60].

The experimental analysis has been carried out in two phases. In the first phase, the influence of the thickness of the coating layer on the value of the friction coefficient has been analysed and the best value of the coating layer thickness has been selected. To this scope, experimental tests have been carried out on specimens with different values of the thickness of the sprayed aluminium coating. Successively, in the second phase, additional tests have been carried out only on the selected interface to evaluate also the influence of the applied pressure on the friction coefficient.

In particular, in the first phase, three different values of the coating thickness have been considered *(50 $\mu m$, 150 $\mu m$ and 300 $\mu m$)* by adopting for each one, two different loading sequences as reported in Table 1. The torque has been assumed equal to 200 Nm and it has been applied by means of a calibrated torque wrench, in order to achieve the desired bolt preloading as described in Section 2.1. In the second phase, other two tests have been performed only on the interface with coating thickness equal to *300 $\mu m$* considering other two values of the tightening torque equal to *300 Nm* and *400 Nm*. The tightening was applied consistently with the European practice choosing among the possible available procedures (torque, combined, HRC or DTI) the torque method, which is the only one that allows to tighten the bolts at values of the clamping force which are lower than the proof preload corresponding to the 70% of the bolt nominal resistance. In fact, while with the combined method, HRC bolts and DTI washers it is possible to control only that the proof preload is achieved, with the torque method intermediate values of the clamping force can be applied not losing accuracy. This is due, as explained in higher detail in Section 2.1, to the linear relationship that exists between torque and clamping force. More details on the accuracy of the tightening procedure when applied to friction dampers are given in [61].

***Table 1:*** *Summary of the tests carried out in the experimental programme*

| ***Coating Thickness*** | ***Number of tightened bolts*** | ***Bolt Torque*** | ***Number of Cycles of the loading sequence*** | ***Amplitude*** |
|---|---|---|---|---|
| 50 μm | *4* | 200 Nm | 10 | +/-15 mm |
| | *8* | | 45 | |
| 150 μm | *4* | 200 Nm | 10 | +/- 15 mm |
| | *8* | | 45 | |
| 300 μm | *4* | 200 Nm | 10 | +/- 15 mm |
| | *8* | 200 Nm | 20 | |
| | *4* | 300 Nm | 10 | |
| | *4* | 400 Nm | 10 | |

## 2.1 TESTS ON THE COMPONENT

The main goals of the experimental campaign are, on one hand, the evaluation of the friction coefficient for different values of the normal force acting on the sliding interface and, on the other hand, the assessment of the cyclic response in terms of stability of the cycles obtained and energy dissipation capacity. In the following the test results are discussed reporting the values obtained for the friction coefficient, determined as:

$$\mu = \frac{F}{n_s n_b\, N_b} \tag{1}$$

where $n_s$ is the number of surfaces in contact, $n_b$ is the number of bolts, $N_b$ is the bolt preloading force and $F$ is the sliding force. In particular, the bolt preloading force $N_b$ is determined starting from the knowledge of the tightening torque by means of the following expression:

$$N_b = \frac{T_b}{k\, d_b} \tag{2}$$

where $T_b$ is the value of the tightening torque, $k$ is a factor accounting for the friction arising between the bolt nut and the plate and between the threads of the bolt shank and nut and $d_b$ is the bolt nominal diameter. In agreement with [54] the value of $k$ has been assumed equal to 0.20.

Even though it is common practice to derive the friction coefficient of such devices by means of Eq. (1), it is useful to note that, according to EN 1993-1-8 [18], the design slip resistance has to be computed as:

$$F_{s,Rd} = \frac{k_s n_s n_b N_b}{\gamma_{M3}} \tag{3}$$

where $\gamma_{M3}$ is the partial safety factor, to be assumed equal to 1.25 for ultimate limit states and equal to 1.10 for serviceability limit states, and $k_s$ is a coefficient accounting for the hole typology. In particular, in case of long slotted holes (i.e. with clearance on the length at least equal to *1.5d* [55]) with the axes of the slot parallel to the direction of load transfer, the value $k_s$=0.63 is suggested.

*2.1.1 Tests with variable thickness of the coating layer*

In order to evaluate the slip resistance of aluminium sprayed surfaces, sliding on steel, characterized by a different value of the coating thickness, different tests have been carried out. As a synthesis of the results, some of the tests and the values of the friction coefficient versus the cumulated displacement are delivered in Fig. 4, with reference to the group of specimens of the 2nd loading sequence. The results obtained are summarized in Table 2.

***1st Loading Sequence***

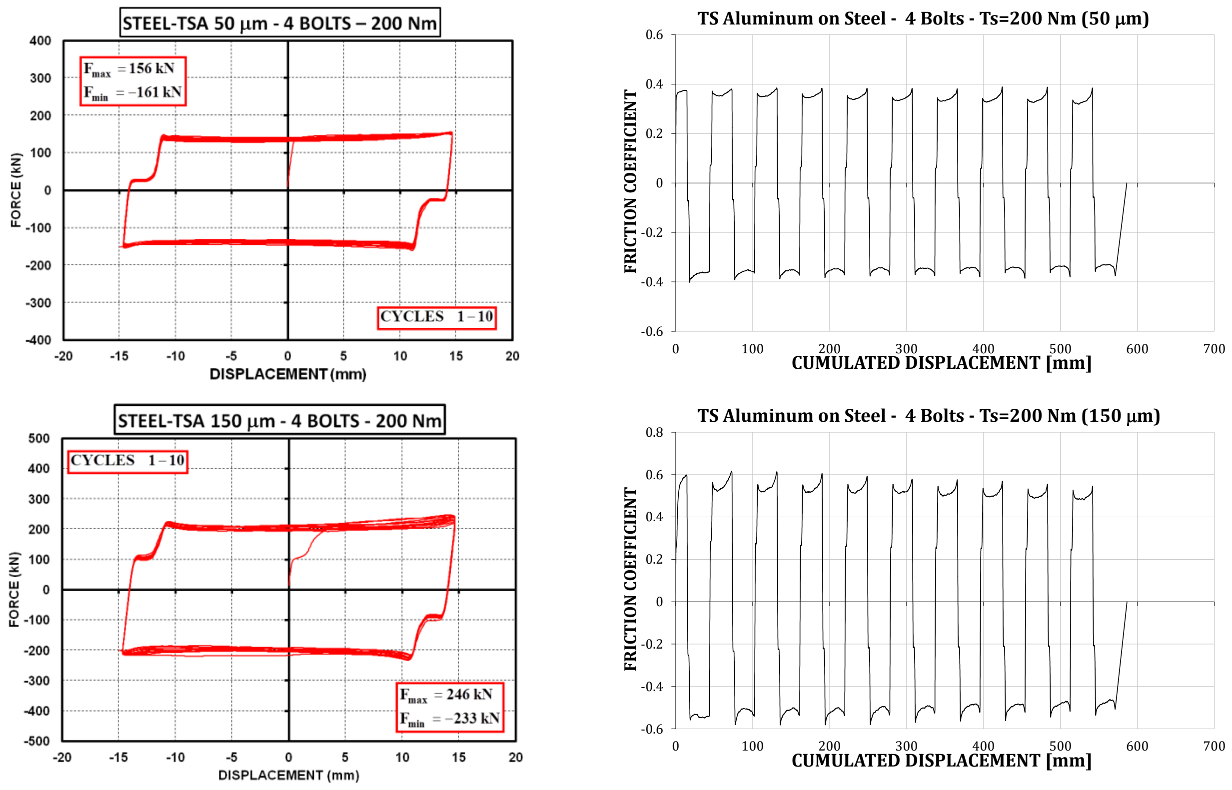

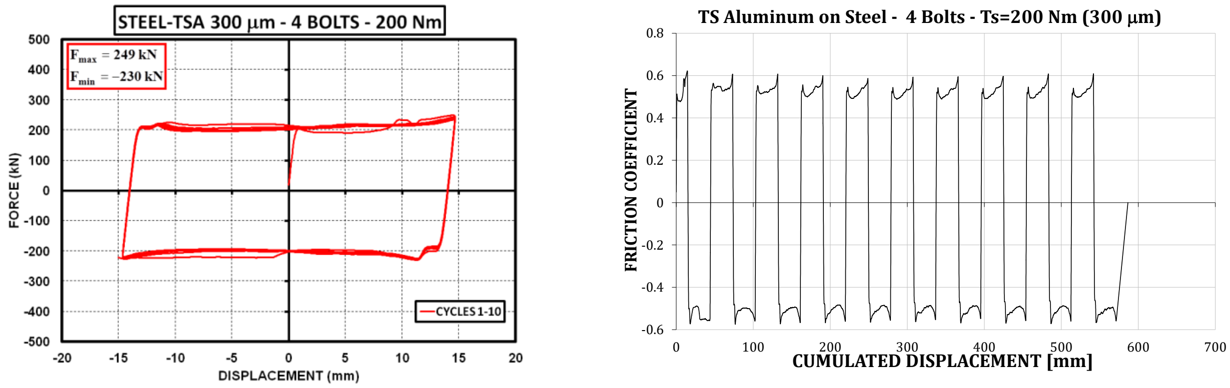


## *2nd Loading Sequence*

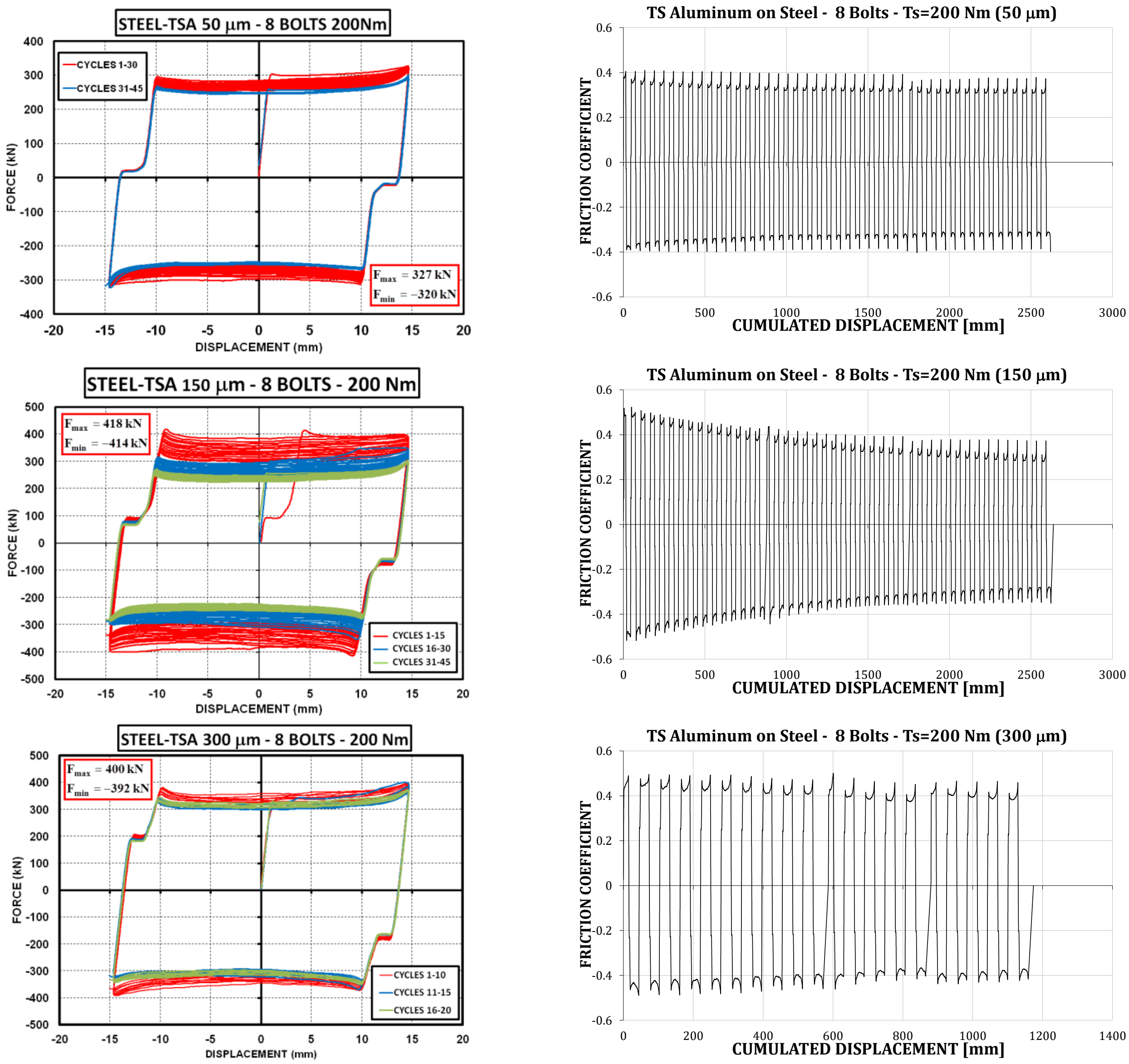


***Figure 4:*** *Results obtained with coatings having different thickness*

The results of the tests point out that the behaviour of all the interfaces is quite stable. All the interfaces exhibited a high initial stiffness and, after reaching the sliding force, began to slide with a force similar to the initial one, evidencing that there is not a significant difference between the static and kinetic coefficient of friction.

It useful to note that the displacements given in Fig. 4 are total displacements including also the elastic contribution due to the axial stiffness of the plate elements constituting the specimens.

In addition, after the first cycle, all the subsequent cycles reached a value of the maximum force slightly lower than the initial one, evidencing the role played by the wearing of the friction material of the coated surface (Fig. 5). However, regarding the degradation of the slip resistance occurring as far as the cumulated displacement increases, it is useful to point out that, in case of destructive seismic events, the friction dampers equipping beam-to-column connections are expected to be subjected to cumulated displacement of about 250 mm [56], so that the degradation pointed out in Fig. 4 can occur only in case of repeated earthquakes.

Analyzing the results summarized in Table 2, it is possible to observe that, considering all the tested interfaces, the value of the friction coefficient ranges in between 0.37 and 0.59, revealing that thermally sprayed aluminium is able to provide a value of the coefficient of friction higher than the metallic and rubber interfaces tested in past experimental investigations [46]. In particular, the highest value of the friction coefficient was obtained with the thickness of 150 μm and the lowest with the thickness of 50 μm.

In addition, the reported tests show that the degradation of the sliding force significantly depends on the thickness of aluminium coating. In fact, considering the first loading sequence (Table 2), in case of 50 μm and 300 μm thickness, the degradation of the sliding force is very low and the ratio between the initial and final friction coefficient is equal to 1.12 and 1.02 respectively. In the first case, probably the result is due to the lower sliding force that provided a limited consumption of the friction pad. Conversely, a higher degradation was shown by the 150 μm interface, whose initial/final sliding force ratio was equal to 1.22. Therefore, analyzing the results on these tests, for the subsequent phase of the experimental work, only the coating with thickness of 300 μm has been considered. In fact, as a result of the first phase tests, this thickness of the coating layer is believed to provide a good compromise between the initial value of friction coefficient and degradation of the sliding force during a cyclic loading history.

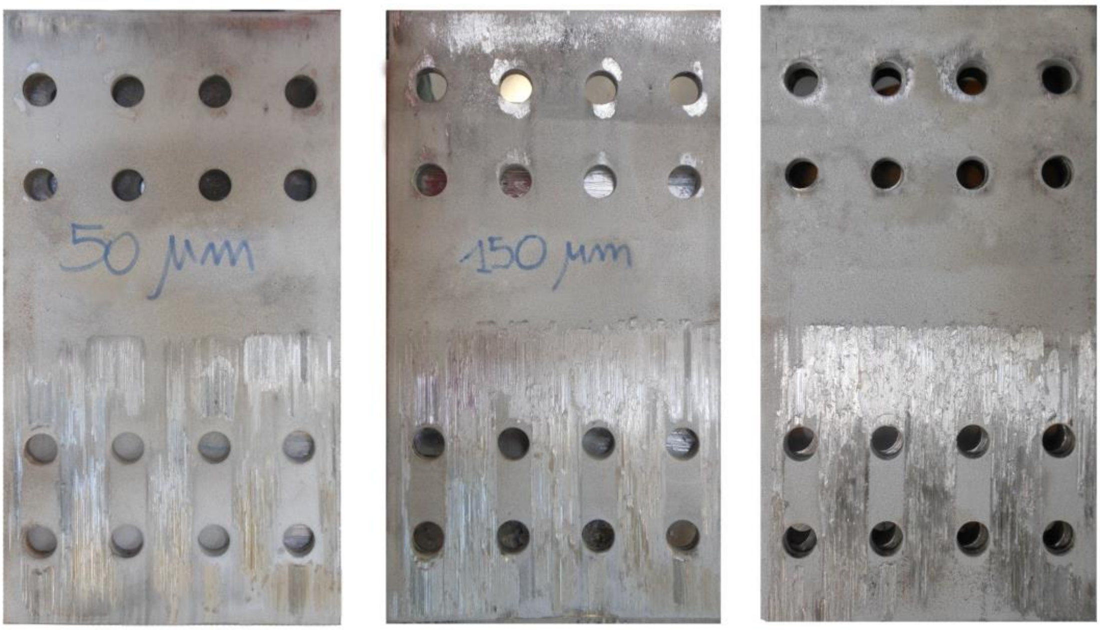


***Figure 5:*** *Appearance of surface of friction pads after testing*

***Table 2:*** *Friction coefficients obtained for different coating thickness*

| **Thickness of the coating** | **1st loading sequence** | | **2nd loading sequence** | |
|---|---|---|---|---|
| | *Initial* | *Final* | *Initial* | *Final* |
| 50 μm | 0.37 | 0.33 | 0.37 | 0.31 |
| 150 μm | 0.59 | 0.48 | 0.52 | 0.29 |
| 300 μm | 0.52 | 0.51 | 0.45 | 0.37 |

Regarding the values of the friction coefficient obtained, it is useful to note that the values given in Table 2 could seem comparable with those which can be obtained by means of shot blasted steel, so that the incentive in using sprayed aluminium could seem not much. As an example, a recent experimental program dealing with the design of slip resistance lap joints [57] has shown, in case of normal holes, a friction coefficient equal to 0.56 in case of joints made of S275 steel whose surface is blasted with shot steel to Sa $2^{1/2}$ and equal to 0.52 in case of joints made of S275 steel whose surface is blasted with shot steel to Sa 3 and spray-metalized with 75 μm zinc. However, it has to be considered that the values given in Table 2 are obtained for long slotted holes, so that they are also the result of a smaller contact area leading to higher local pressures. The influence of the hole typology is accounted for by means of the coefficient $k_s$ in Eq. (3) which, according to Eurocode 3, is equal to 0.63 aiming to provide a safe side value of the slip resistance. According to [58], such influence is about 30% in case of long slotted holes, so that the value 0.59 obtained in case of 150 μm coating thickness is equivalent to a value of about 0.77 for normal holes. This consideration points out the advantage which can be obtained by means of thermally sprayed aluminium.

Moreover, it is useful to note that values of the friction coefficient higher than those obtained in the experimental tests herein presented have been obtained by other researchers [48]. This difference can be attributed to the differences in the preliminary treatments applied before thermal spraying and/or to the main setting parameters of the machine employed to apply the coatings, i.e. the amperage, voltage and pressure of the air, which have to be changed according to the melting temperature of the materials applied.

### *2.1.2 Tests with variable pressure*

As aforesaid, in order to evaluate the influence of the tightening pressure on the value of the slip resistance, additional tests have been carried on further specimens having the selected coating thickness. In particular, three different values of the tightening torque have been considered and only one loading sequence of ten cycles with amplitude of +/- 15 mm has been adopted. The behaviour exhibited by such specimens is reported in Fig. 6. It evidences a response very similar to that reported in previous tests, but reveals that the value of the initial coefficient of friction, for this interface, is also affected by the pressure applied on the interface. In fact, as it is possible to observe, as far as the value of the tightening torque increases, the initial friction coefficient decreases (Fig. 7).

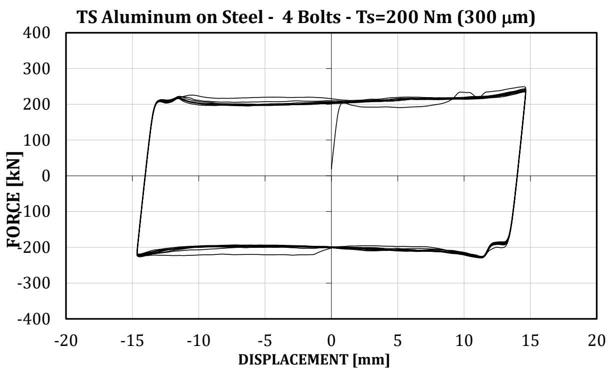


*(Ts=200Nm)*

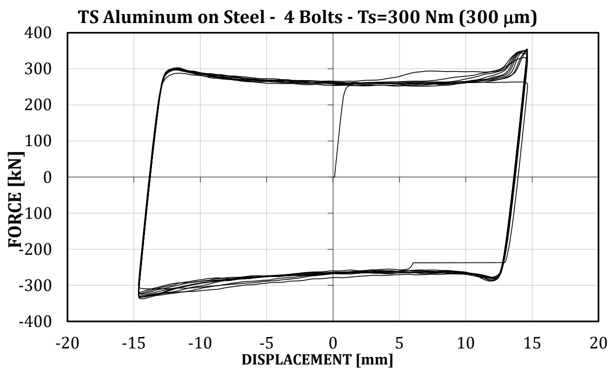


*(Ts=300Nm)*

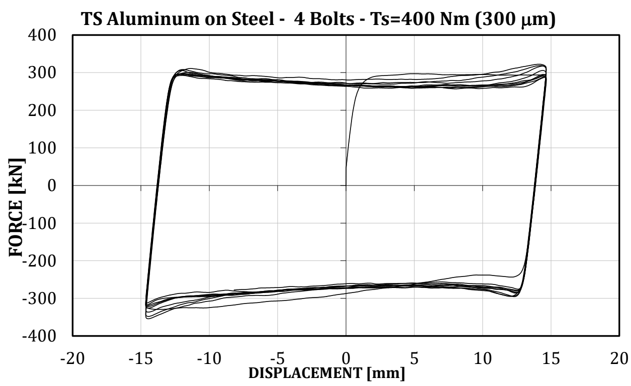


*(Ts=400Nm)*

*Figure 6:* *Cyclic response for different values of the applied tightening torque*

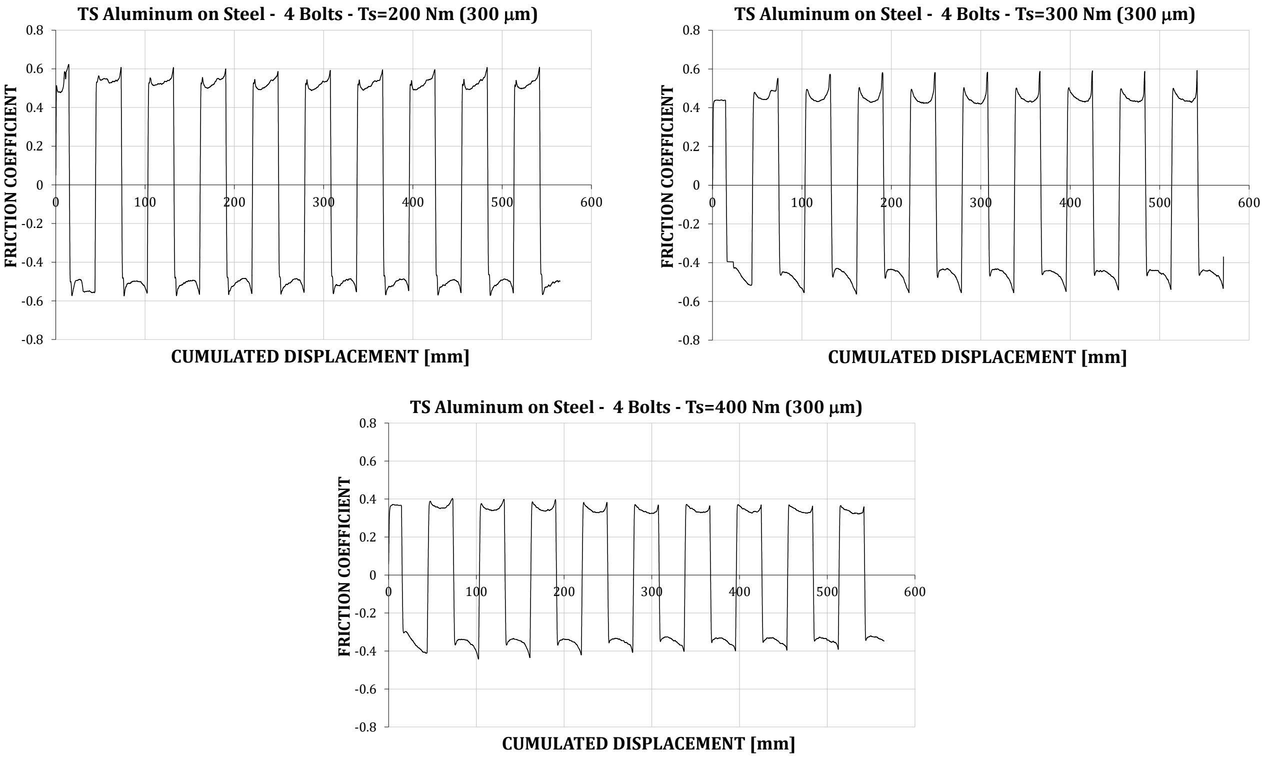


***Figure 7:*** *Friction coefficient vs. cumulated displacement for different tightening levels*

Therefore, in order to develop a mechanical model to design beam-to-column connections equipped with friction dampers with thermally sprayed aluminium pads, a relationship providing the initial friction coefficient as a function of the pressure applied at the interface has been derived. To this scope, the pressure applied at the interface has been estimated assuming that the normal force is transferred by the bolts to the plates spreading with a slope equal to 45°, obtaining the following equation which includes the influence of the long slotted hole (Fig. 8):

$$p = \frac{4N_b}{\pi \xi^2 d_b^2 \left(1 - 2\frac{\arcsin(\eta/\xi)}{\pi} - \frac{\eta}{\pi\xi}\sqrt{1-\left(\frac{\eta}{\xi}\right)^2}\right)^2} \tag{4}$$

where $\eta d_b$ is the slot width and:

$$\xi = \frac{d_{bh} + 2\left(t_w + t_p + t_{fp}\right)}{d_b} \tag{5}$$

being $d_b$ the bolt diameter, $d_{bh}$ the bolt head diameter, $t_w$ the washer thickness, $t_p$ the outer plate thickness and $t_{fp}$ the friction pad thickness.

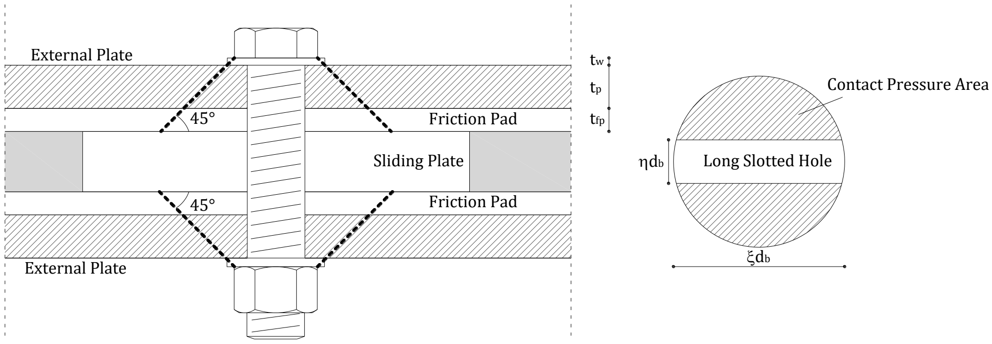


***Figure 8:*** *Assumed geometry of the contact pressure area*

It is useful to note that the above relationships are valid provided that the distance between the slots and the bolt pitch is greater than $\xi d_b$ and, in addition, the distance between the slot and the plate edge is greater than $\xi d_b/2$. When such conditions are not satisfied the interaction has to be accounted for. In Fig. 9 the result of the regression analysis of the experimental data is reported. Nevertheless, being referred only to three experimental data, this regression has to be considered with some caution.

The influence of the pressure on the friction coefficient is justified considering that all surfaces are rough on a microscopic scale and real contact is obtained over a small fraction of the apparent contact area. Friction is related to the real contact area and independent of the apparent contact area. Real contact area is affected by the applied pressure which, therefore, affects the resulting friction coefficient. In particular, the increase of the applied pressure tends, on one hand, to flatten the surface asperities, thus reducing the amount of friction due to the mechanism of asperity interlocking and, on the other hand, to increase the real contact area thus improving the adhesion mechanism. The prevailing between these two phenomena will govern the dependence of the friction coefficient on pressure and can be investigated by experimental results only.

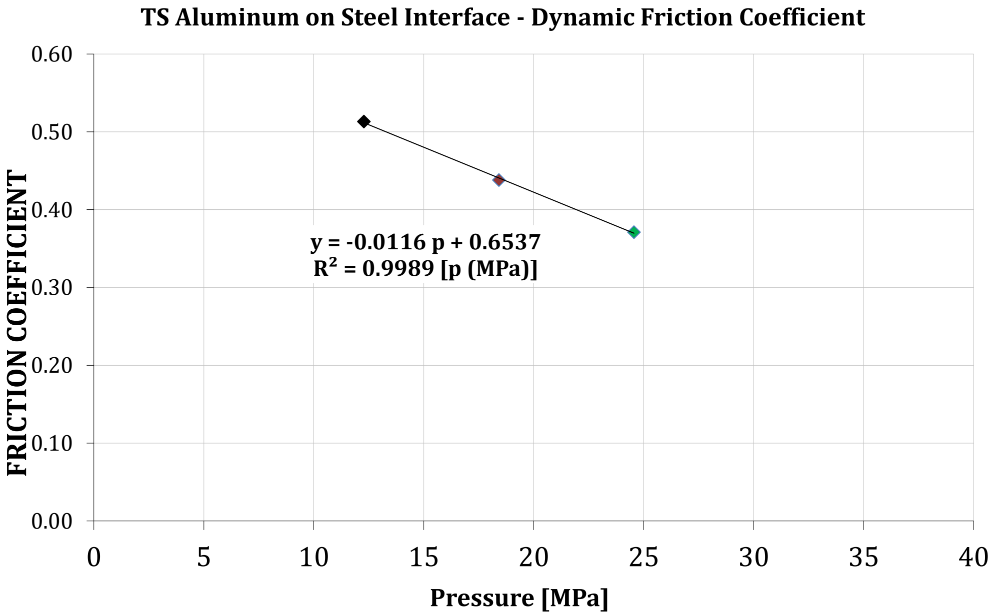


***Figure 9:*** *Influence of the contact pressure on the friction coefficient*

## 3 CONCEPT AND DESIGN OF TESTED SPECIMENS

Starting from the above results, the design of dissipative connections equipped with friction dampers was performed. The joint detail proposed in this paper is the modification of the classical detail of a double split tee beam-to-column connection obtained by connecting the beam bottom flange to the column flange by means of three steel angles, composed by welding, and by interposing between them and the beam flange one or two friction pads (Fig. 10). In this way, the energy dissipation supply is provided by the friction damper, while all the other elements of the connection and the beam are designed in order to be free from yielding. Exception has to be made for the stem of T-stub and angles, close to the T-stub flange and vertical angle leg respectively, which in order to accommodate the rotation are subjected to minor yielding. This strategy, as already demonstrated in some preliminary studies on similar prototypes, allows the development of beam-to-column connections with high energy dissipation able to accommodate the required rotations without any significant damage [47]. The classical T-stub connection at the top flange level is aimed to fix the centre of rotation with the goal of preventing the damage to the reinforced concrete slab, while the bottom damper provides, thanks to its stroke, the required rotation capacity and the energy dissipation.

A significant advantage of this joint configuration is that, by controlling the tightening torque applied to the bolts, it is possible to calibrate magnitude of the sliding resistance of the friction damper and, therefore, depending on the lever arm, the magnitude of the bending moment transmitted to the column. It is useful to note that, in order to assure that the beam end remains in elastic range, the bending sliding resistance of the connection has to be not greater than the nominal bending resistance of the connected beam. However, in order to maximize the exploitation of the beam under gravity loads and under the internal actions occurring when the structure is subjected to horizontal forces corresponding to serviceability limit states, such as wind actions or frequent seismic events having a low return period, the ratio between the bending sliding resistance of the connection and the nominal bending resistance of the connected beam has to be as close as possible to 1.0. In order to satisfy the above design criterion and to maximize the exploitation of the connected beam, the use of a beam end haunch to increase and calibrate the lever arm can also be suggested (Fig. 11). In such a way, the beam section is fully exploited, but both the oversizing of the other joint components (such as the panel zone usually requiring supplementary web plates, the beam end requiring reinforcing ribs or cover plates, the increase of the bolt diameter, etc.) and the column oversizing (because of beam-column hierarchy criterion) can be significantly limited and/or controlled.

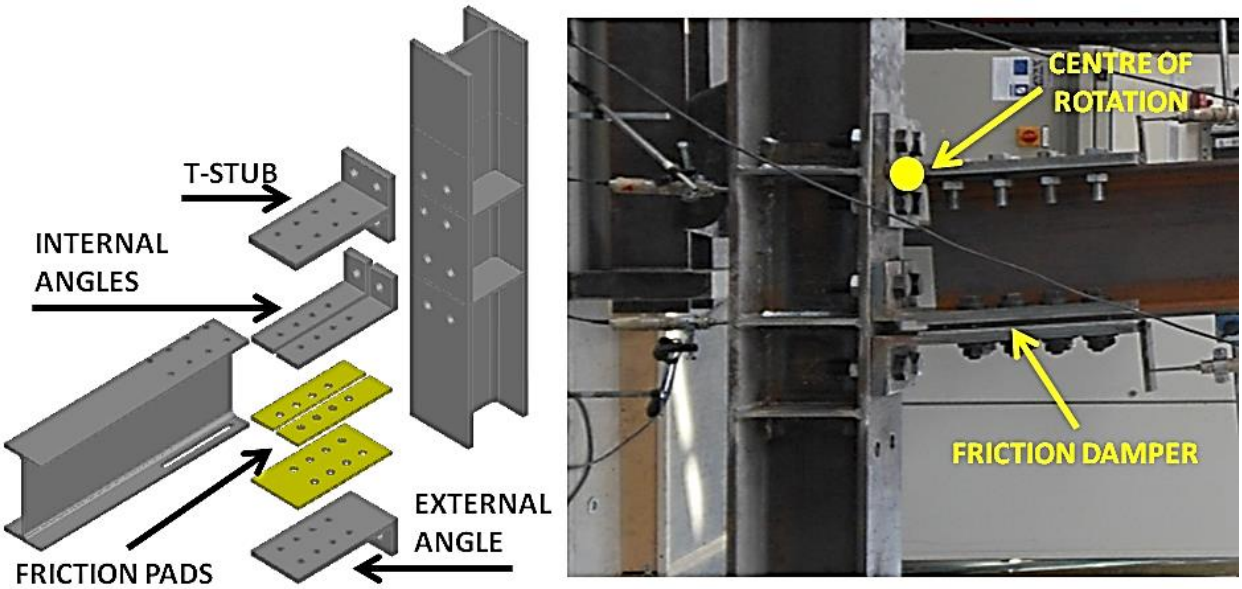


***Figure 10:*** *Beam-to-column connection equipped with friction dampers*

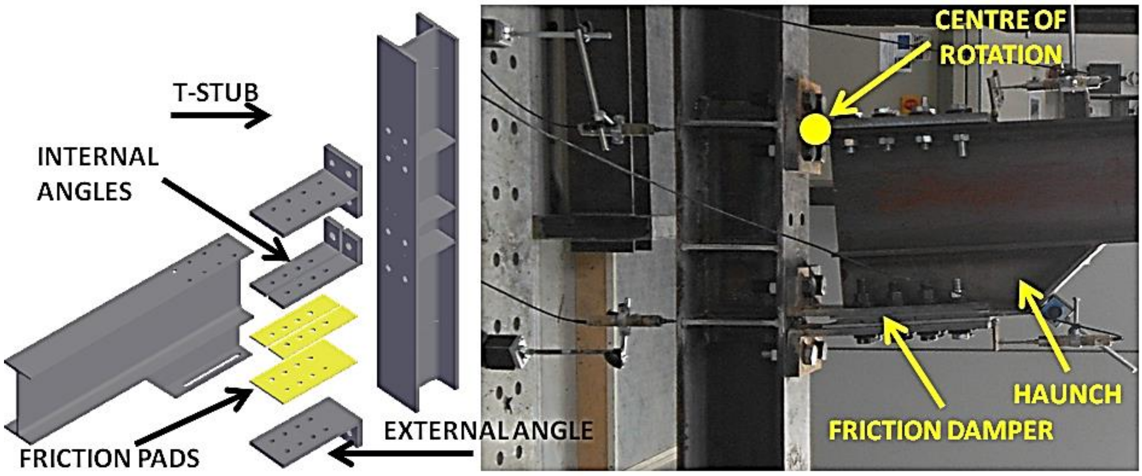


**Figure 11:** *Beam-to-column connection equipped with friction dampers and additional haunch*

Within the experimental activity described in this paper two different joints equipped with the friction damper previously tested under uniaxial loading conditions were tested under cyclic loading conditions. In particular, the two joints fasten an IPE270 beam to an HEB200 column, both of them made of S275 steel. They are identified as follows:

- ***TSJ-SA300-320-CYC12:*** it is a joint where the upper beam flange is connected to the column by means of a T-stub, while the lower beam flange is fastened to the column by means of a system of three angles (Fig. 10). Three steel plates with a 300 μm coating of thermally sprayed aluminium are located in between the beam flange and the angles in order to realize the friction damper;
- ***TSJ-H-SA300-260-CYC13:*** it is a joint with a detail very similar to the previous one where, in order to increase the lever arm, the friction damper is applied by means of an additional haunch which is welded to the beam. This allows the reduction of the tightening torque and/or of the number of bolts (Fig. 11).

Starting from the values of the friction coefficients derived in previous section, the design of the dissipative connections equipped with friction pads was performed. Within the framework of the component method, the following components have to be designed: the shear panel, the column web panels in tension and compression, the T-stub/angles and the friction damper. In order to obtain a joint where the only component providing energy dissipation is the friction damper, the steel parts have to possess sufficient overstrength with respect to the maximum force that the friction damper is able to transmit. According to this hierarchy, the geometry of all the elements composing the joint was defined by exploiting the formulations provided by literature models or by means of the formulations given in Eurocode 3 [17].

Specimen TSJ-SA300-320-CYC12 was designed to develop a bending moment evaluated at the level of the column face equal to the beam nominal plastic resistance (133 kNm). It means that the joint was designed to assure that the beam end remains in elastic range. In fact, considering that the friction damper is characterized by a rigid-plastic response, imposing that the slip resistance of the damper occurs at the attainment of a bending moment equal to the characteristic flexural resistance of the beam, assures that the connected member remains elastic. A similar criterion has been adopted for specimen TSJ-H-SA300-260-CYC13 accounting, however, for the possibility to increase the slip resistance of the connection beyond the nominal resistance of the beam evaluated at the column face. In fact, in this case, it is possible to account for the increase of resistance of the beam in the haunched part increasing, consequently, the slip resistance of the damper. Therefore, this joint has been designed to develop a bending moment equal to 1.4 times the beam nominal resistance, namely 187 kNm. Taking into account that the beam length (i.e. the distance between the actuator and the column face) is equal to 1460 mm and that the un-strengthened segment of the beam is equal to 885 mm, when the design bending moment at the column face is achieved (187 kNm), the bending moment acting at the end of the haunch is equal to $187 \times 885/1460 \cong 113$ kNm (which is about 0.85 times the beam nominal resistance). It means that also for this specimen, when slippage occurs, the bending moment in the un-strengthened portion of the beam is lower than the beam nominal resistance, assuring that it remains elastic. These reference values of the flexural resistance were used to define the tightening torque of the bolts of the friction damper accounting for the friction coefficient values previously reported.

All the remaining joint components have been designed with an appropriate overstrength. In particular, the column shear panel has been reinforced with a couple of 10 mm supplementary plates welded on the column web, while the panels in tension and compression have been stiffened with a couple of continuity plates with a thickness equal to the beam flange thickness. However, in order to obtain structural details which are more cost effective the possibility to omit these strengthening elements can be evaluated. In addition, the upper T-stub and the lower angles have been designed in order to remain in elastic range under a force level corresponding to the friction damper design force.

Dealing with the friction damper, the parameters to be controlled in the design are the length of the slots made on the beam flange or on the haunch (which allow the slip of the beam flange on the friction pad) and the tightening torque to be applied to the bolts which are used to preload the friction pads. In particular, the first parameter governs the rotational capacity of the connection and, as a consequence, it can be selected starting from the expected value of the joint rotation ($\phi$) under the most severe design earthquake, by using the following equation:

$$L_{slot} = (n_{br} - 1)p + d_b + 2\phi\, z \tag{6}$$

where $d_b$ is the bolts diameter, $n_{br}$ is the number of bolt rows used to fasten the stem of the angles to the beam bottom flange, $p$ is the bolt pitch and $z$ is the lever arm. For the tested specimens $d_b$*=20 mm,* $n_{br}$=4, *p=60 mm* and $z$ = 265 mm for specimen TSJ-SA300-320-CYC12 and $z$ = 411 mm for specimen TSJ-H-SA300-260-CYC13, respectively. Therefore, by assuming $\phi$ =0.08 rad, according to this criterion a length of the slot equal to 270 mm has been chosen for the two joints. The clear gap between the beam edge and the inside of the flange of the Tee section has been assumed equal to about two times the thickness of T-stub stem to allow the local yielding required to accommodate the beam rotation.

The second parameter governs the magnitude of the bending moment that the joint is able to withstand before the slippage of the friction damper occurs. In particular, the design force of the friction damper can be easily defined as the design bending moment divided by the lever arm. The design friction resistance of the damper device is equal to 133/0.265≅502 kN in case of specimen TSJ-SA300-320-CYC12 and equal to 187/0.411≅455 kN in case of specimen TSJ-H-SA300-260-CYC 13. Starting from the knowledge of the friction damper design force, exploiting Equations (1) and (2) and the relationship between the friction coefficient and the pressure applied at the interface (Fig. 9), it is possible to determine the value of the tightening torque to be applied, equal to 320 Nm and 260 Nm for the two tested specimens. The details of the specimens are delivered in Fig. 12.

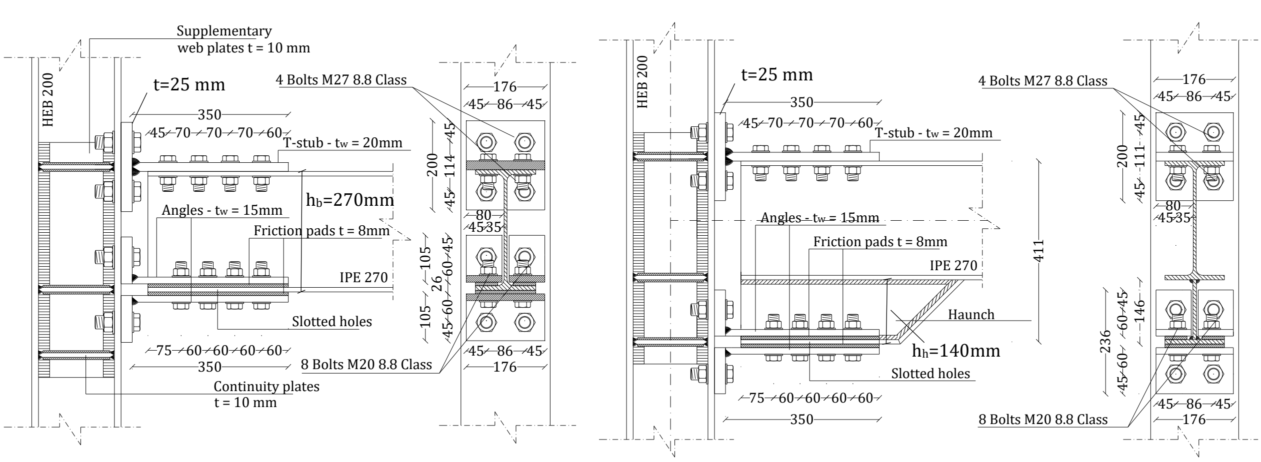


***Figure 12:*** *Details of the tested specimens. Left: TSJ-SA300-320-CYC12; Right: TSJ-SA300-260-CYC13*

## 4 EXPERIMENTAL LAYOUT

The experimental tests were carried out at Materials and Structures Laboratory of Salerno University. Two steel hinges, designed to resist shear actions up to 2000 kN and bolted to the strong floor base beam, were adopted to connect the specimens to the reacting system. The specimens were assembled with the column (HEB 200) in horizontal position, connected to the hinges, and the beam (IPE 270) in vertical position (Fig. 13). The loads were applied by means of two different hydraulic actuators. The first one used to apply, under force control, an axial load in the column equal to 30% of the squash load. The second actuator to apply, under displacement control, the desired displacement history at the beam end. In order to avoid the lateral-torsional buckling of the beam, an horizontal transversal frame was conceived to work as a guide which restraints the lateral displacement of the beam. The loading history was defined in terms of drift angle, according to the testing protocol provided by AISC, 2005 [59].

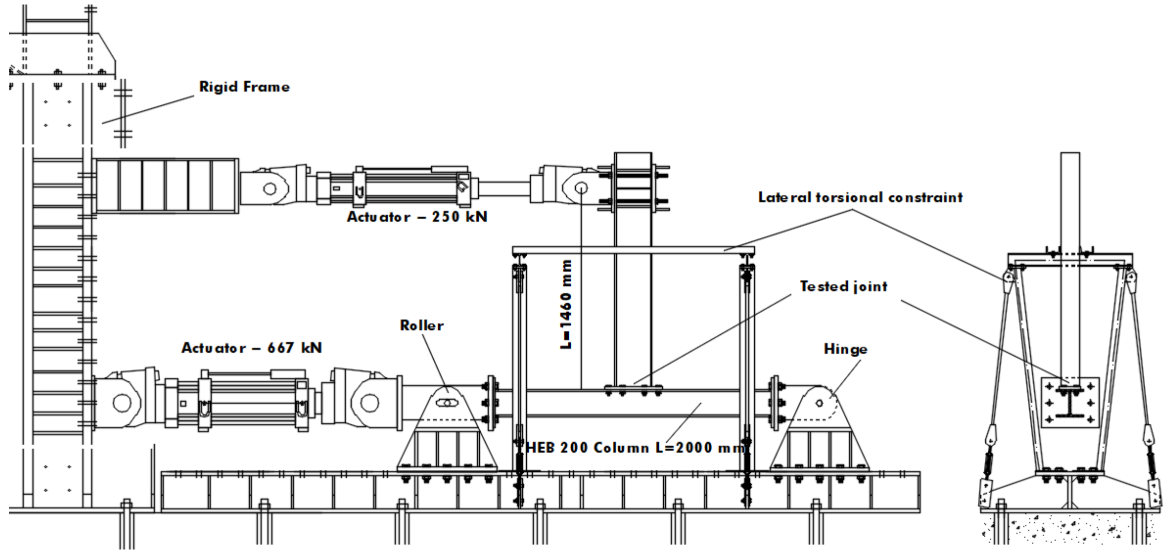


***Figure 13:*** *Experimental layout for tests on joints*

During the tests the displacement history imposed by the top actuator and the displacements of the different joint components were acquired In particular, in each test, four LVDT were used to measure the local displacement of the friction damper, the rotation of the panel zone and to control that the axial displacements exhibited by the fixed T-stub were negligible (Fig. 14).

Aiming at the evaluation of the beam end displacements due to the beam-to-column joint rotation only, the top displacements of the cantilever beam measured by means of the LVDT equipping the actuator were corrected by subtracting the elastic contribution due to the beam and column flexural deformability according to the following relationship:

$$\delta_j = \delta_{MTS} - \frac{FL_b^3}{3EI_b} - \frac{FL_cL_b^2}{12EI_c}\left[\left(\frac{L_c}{L_c+2a}\right)^2 + \frac{6a}{L_c+2a}\right] \qquad (7)$$

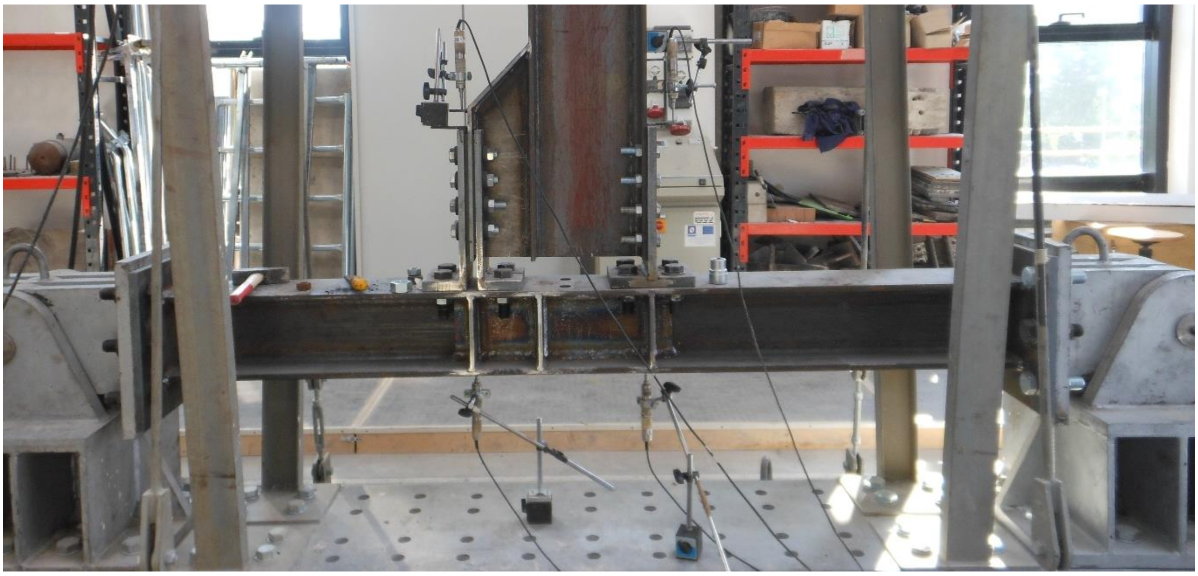

***Figure 14:*** *Position of LVDTs used to measure the local displacements*

where $\delta_{MTS}$ is the overall top horizontal displacement evaluated at the level of MTS actuator, $I_b$ and $I_c$ are the beam and column inertia moments, $L_c$ is the column length, $L_b$ is the beam length and $a$ is the length of the rigid parts, due to the steel hinges (Fig. 15).

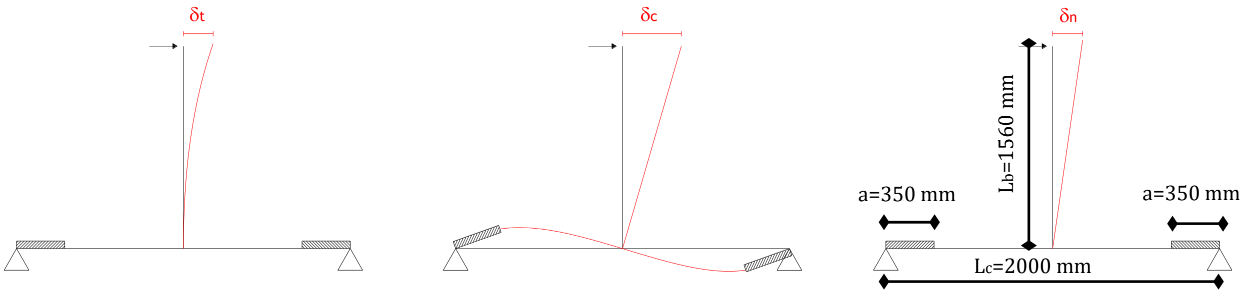


*a) beam contribution* *b) column contribution* *c) joint contribution*

***Figure 15:*** *Scheme for evaluating the joint contributions to the overall top displacement*

The identification label of the tests refers to the following issues: 1- Joint typology, i.e. Tee Stub Joint (TSJ) or Tee Stub Joint with haunch (TSJ-H) / 2 – Friction interface, i.e. SA300 (Sprayed Aluminium with 300 μm coating) / 3 – Tightening torque of the bolts in Nm / 4 – Progressive number of cyclic tests, i.e. CYCXX.

## 5 CYCLIC BEHAVIOR OF SPECIMENS

As aforesaid, the two joints (Fig. 16) were tested under cyclic loading conditions following the drift history suggested by the AISC loading protocol. As expected, on the basis of the design criteria adopted, in all the experimental tests there has not been any significant damage of the joint components, but only the wearing of the friction pads. Therefore, a very important outcome of the experimental program is the verification that this connection typology can be subjected to repeated cyclic rotation histories, i.e. to repeated earthquakes, by only substituting the friction pads, if needed, and by tightening again the bolts to reach the desired preloading level. In addition, the rotation capacity can be easily calibrated by simply governing the length of the slotted holes. In fact, in all the tests the rotation demand applied to the joint has been completely due to the slippage of the friction damper located at the bottom beam flange. The experimental results are in line with the outcomes of the tests on the friction interfaces pointing out that, as expected, the cyclic behaviour of the joint is mainly governed by the cyclic behaviour of the weakest joint component, i.e. the friction damper.

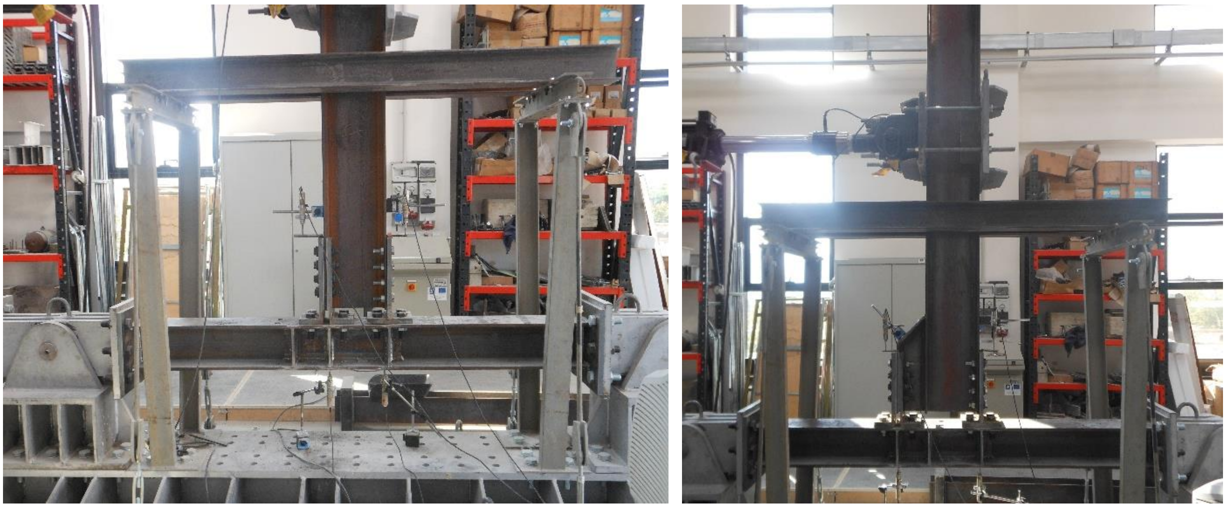

***Figure 16**: Specimens before testing*

In fact, in both tests the response has been very similar to that exhibited during the uniaxial tests on the interface. At low force values the joints exhibited an elastic behaviour characterized by a high initial stiffness. In particular, in case of joint TS-H-SA300-260-CYC13 the initial stiffness was sensibly higher due to the increased lever arm provided by the additional haunch. When the force applied at the end of the cantilever beam reached a value approximately equal to the design bending moment divided by the beam length, the slippage of the friction dampers started (Figs. 17-18). After the first slippage, the joints hysteretic response was characterized for all the loading/unloading cycles approximately by a parallelogram shape with a slight strength degradation as the number of the cycles of the loading history increases (Fig. 19).

By the comparison with the results of the tests carried out on the friction dampers (i.e. the component alone), it is worth noting that the main difference between the hysteresis cycles of the friction DST joint and those observed during the uniaxial tension test is the asymmetric response. This difference is mainly due to the role played by the beam rotation in the kinematic mechanism. In fact, the beam rotation causes two effects that give rise to an increase of the bending moment as far as the beam rotation increases. On one hand, there is an increase of the local pressure on the friction pads due to the reaction force provided by the stem of the fixed T-stub at the top beam flange level and by the stems of the angles at the bottom flange level, that behave in a way similar to a pocket foundation. Because of this pocket foundation effect, the increase of the pressure on the friction pads depends on the direction of the horizontal displacement of the cantilever. Therefore, the asymmetry of the cyclic response is due to the reduction of the friction coefficient when the pressure on the friction pads increases. Additionally, when the dampers are in tension a deformation of the steel angles occurs, probably providing a reduction of the bolt forces due to the opening of a small gap in the web plates. On the other hand, minor yielding of the tee stems at the stem-to-flange connection of top T-stub and bottom angles contributes to the total bending resistance providing a slight hardening behaviour as experimentally observed (Fig. 19).

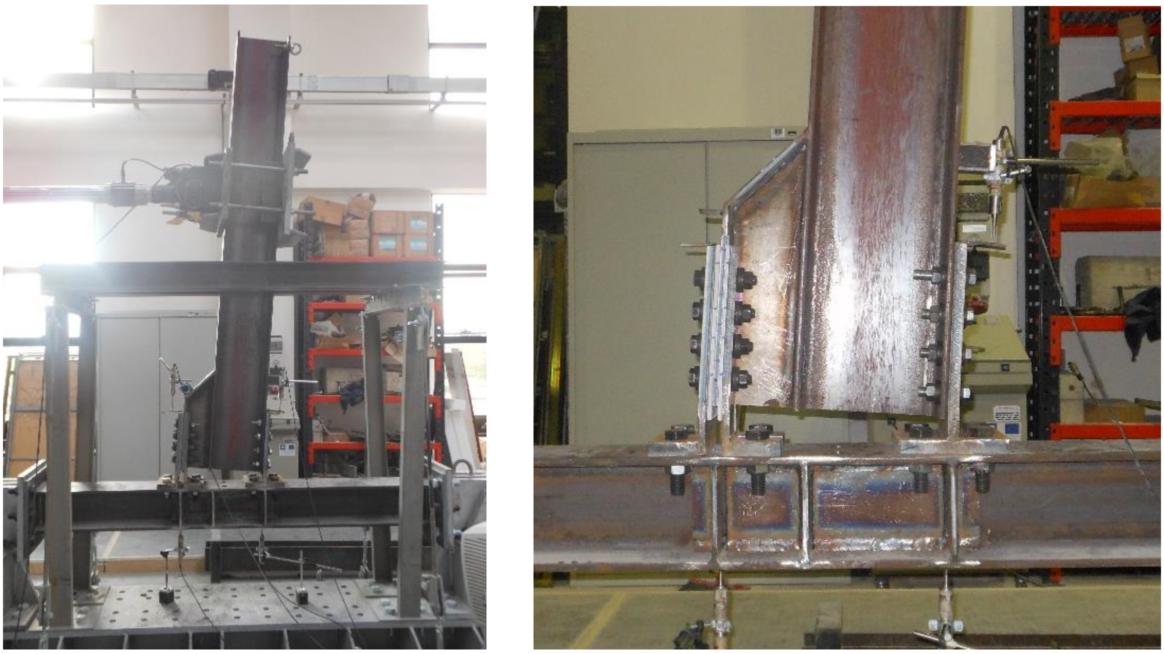

***Figure 17****: Sliding motion of the friction damper*

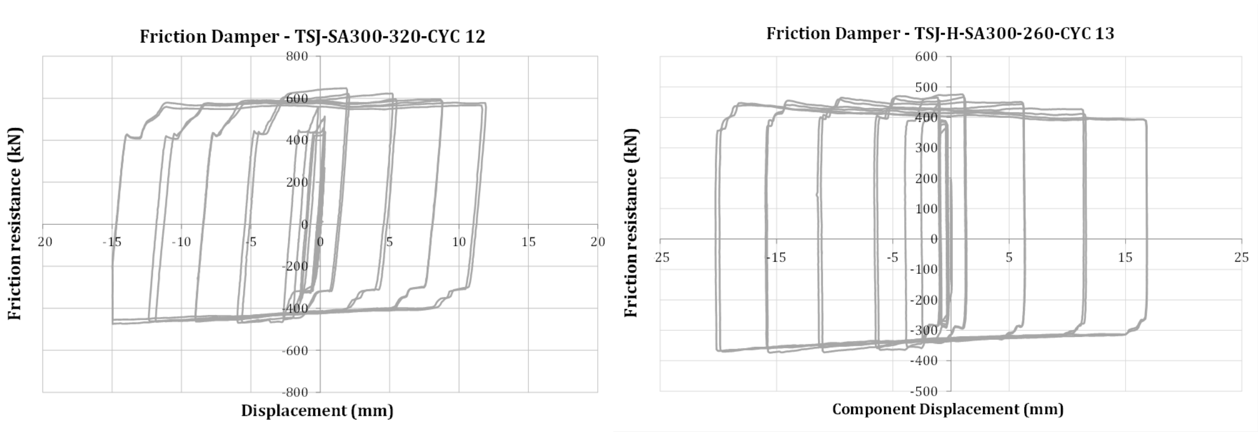


***Figure 18**: Force-Displacement response of the friction dampers*

The most important feature of the proposed connection is that, as confirmed by the experimental results, it is able to provide a high dissipative capacity also under values of the rotation significantly greater than the minimum value, equal to 35 mrad, required by Eurocode 8 [1] for frames in High Ductility Class. Furthermore, it is possible to observe from Fig. 18 and Fig. 19 that the resistances of the joints and of the dampers approximately correspond to the design ones, confirming the accuracy of the design procedure previously described. Finally, it is very important to underline that the obtained flexural strength is greater than the plastic resistance of the connected beam, so that practically full-strength connections are obtained without providing any damage to the beam ends. This is highlighted in Fig.19 reporting with dashed lines the bending moment corresponding to the nominal beam resistance. In particular, it is worth to observe that even though no damage was detected in the elements of the connection or in the members, the nominal bending resistance of the beam evaluated at the level of the column face was equated or exceeded. This shows that with the proposed connection it is possible to obtain a wide and stable hysteretic behaviour with negligible damage, carrying the same forces that the beam would normally carry with a full-strength connection.

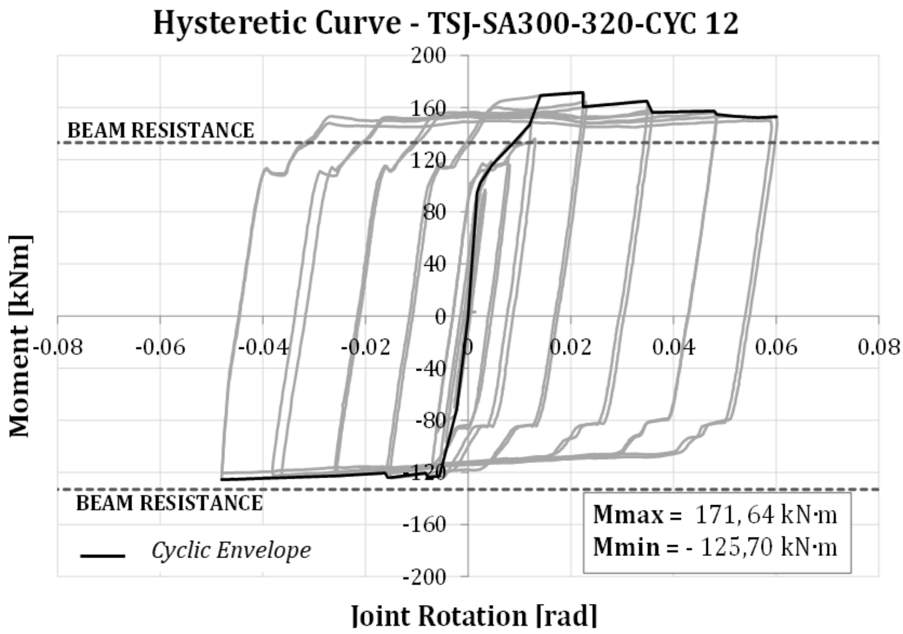


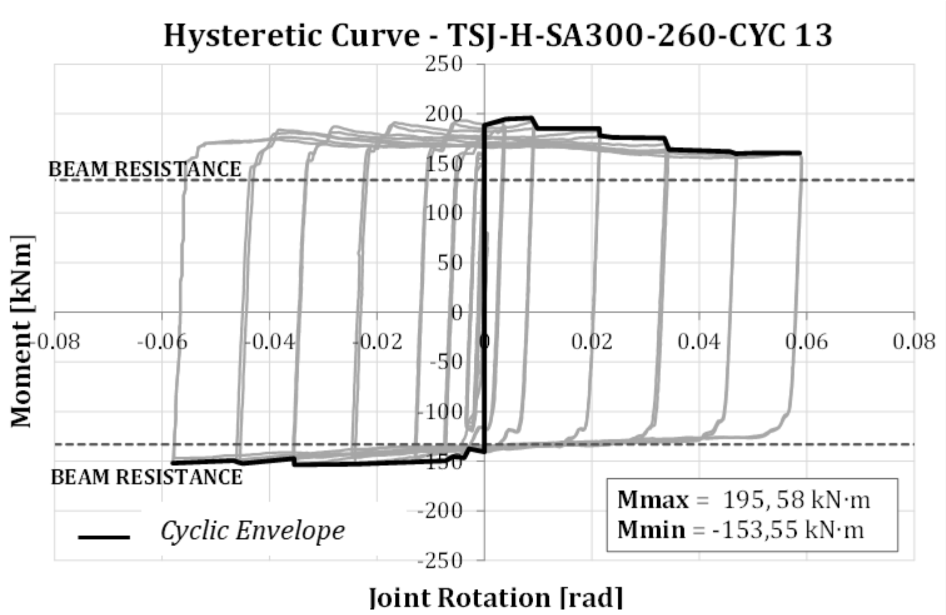


***Figure 19****: Moment-rotation curves of tested joints*

## 6. CONCLUSIONS

The results of an experimental program devoted to evaluate the possibility to equip steel joints with friction dampers realized with pads coated with thermally sprayed aluminium have been presented. The main outcomes of the experimental programs can be summarized as follows:

- The frictional interface "thermally sprayed aluminium on steel" is characterized by good values of the kinematic friction coefficient. In fact, compared to other metallic or rubber materials tested in a past experimental program under the same loading conditions it is able to exhibit greater values of the friction coefficient;

- The thermally sprayed aluminium has, among the various advantages, the benefit to be an economic material compared to rubbers or other metals typically used for tribological applications such as brass;
- The friction coefficient of the interface decreases as far as the pressure applied to the interface increases. Therefore, in order to develop high values of the sliding force it is advisable to limit the pressure applied on the frictional material, as an example by increasing the number of the bolts thus allowing the reduction of their tightening torque;
- The results of the experimental program on the friction damper have shown that a good balance between the initial value of the friction coefficient and the degradation of the sliding force during a cyclic loading history can be reached with a thickness of aluminium coating equal to 300 μm;
- As the bolt preloading has not been directly measured and monitored throughout the tests, it is not possible to quantify in detail the actual value of the friction coefficient and its evolution during the tests. Notwithstanding, the overall sliding resistance of the damper is accurate as directly measured in the components' tests and derived as the ratio between the sliding flexural resistance and the lever arm in the tests on beam-to-column connections. This force is directly affected by the tightening torque;
- For the above reasons, new experimental tests are currently in progress where the bolt preloading is continuously measured by means of annular load cells.

**ACKNOWLEDGEMENTS**

The research activity herein presented has been supported by the European Community by research grant RFSR-CT-2015-00022. The support of the European Commission within RFCS Research & Innovation is gratefully acknowledged.

## REFERENCES

1. CEN. Eurocode 8: Design of structures for earthquake resistance - Part 1: General rules, seismic actions and rules for buildings; 2005a.

2. D'Aniello M., Tartaglia R., Costanzo S., Landolfo R. (2017). Seismic design of extended stiffened end-plate joints in the framework of Eurocodes. Journal of Constructional Steel Research, Volume 128, January 2017, Pages 512–527.
3. Piluso V, Rizzano G. Random Material Variability effects on Full-strength end-plate Beam-to-Column Joints. Journal of Constructional Steel Research. 2007;63(5):658-666.
4. Latour M, Rizzano G. Full Strength Design of Column Base Connections accounting for Random Material Variability. Engineering Structures. 2013;48:458-471.
5. Mazzolani F, Piluso V. Theory and Design of Seismic Resistant Steel Frames. London: E & FN Spon, an Imprint of Chapman & Hall; 1996.
6. D'Aniello M, Landolfo R, Piluso V, Rizzano G. Ultimate behavior of steel beams under non-uniform bending. Journal of Constructional Steel Research. 2012;78:144-158.
7. Grecea D, Dinu F, Dubina D. Performance Criteria for MR Steel Frames in Seismic Zones. Journal of Constructional Steel Research. 2004;60:739-749.
8. Carter CJ, Iwankiw N. Improved ductility in seismic steel moment frames with dogbone connections. Journal of Constructional Steel Research. 1998;46(1-3):253.
9. Engelhardt MD, Winneberger T, Zekany AJ, Potyraj TJ. Experimental investigation of dogbone moment connections. Paper presented at: Proceedings of National Steel Construction Conference, 1997; Chicago.
10. Montuori R., Nastri E., Piluso V., Troisi M. Influence of connection typology on seismic response of MR-Frames with and without 'set-backs'. Earthquake Engineering & Structural Dynamics. 2017; 46 (1), 5-25.
11. Montuori R., Nastri E., Piluso V., Advances in theory of plastic mechanism control: closed form solution for MR-Frames. Earthquake Engineering & Structural Dynamics. 2015; 44 (7), 1035-1054
12. Faella C, Montuori R, Piluso V, Rizzano G. Failure mode control: economy of semi-rigid frames. Paper presented at: Proceedings of the XI European Conference on Earthquake Engineering, 1998; Paris.
13. Tenchini A., D'Aniello M., Rebelo C., Landolfo R., da Silva L.S., Lima L. (2014). Seismic performance of dual-steel moment resisting frames. Journal of

Constructional Steel Research, Volume 101, October 2014, pp. 437-454. DOI:10.1016/j.jcsr.2014.06.007

14. Cassiano D., D'Aniello M., Rebelo C., Landolfo R., da Silva L. (2016). Influence of seismic design rules on the robustness of steel moment resisting frames. Steel and Composite Structures, An International Journal, Volume 21, Number 3, , pp. 479-500, June30 2016
15. Faella C, Piluso V, Rizzano G. Structural Steel Semi-Rigid Connections. Boca Raton: CRC Press; 2000.
16. CEN. Eurocode 3: Design of steel structures - Part 1-1: General rules and rules for buildings; 2005b.
17. CEN. Eurocode 3: Design of steel structures - Part 1-8: Design of joints; 2005c.
18. Cassiano D., D'Aniello M., Rebelo C., (2017) Parametric finite element analyses on flush end-plate joints under column removal. Journal of Constructional Steel Research, Volume 137, October 2017, Pages 77–92
19. Iannone F, Latour M, Piluso V, Rizzano G. Experimental Analysis of Bolted Steel Beam-to-Column Connections: Component Identification. Journal of Earthquake Engineering. 2011;15(2):214-244.
20. Jaspart J, Demonceau J. European Design recommendations for simple joints in steel structures. Journal of Constructional Steel Research. 2008;64/7(8):822-832.
21. Jaspart J, Demonceau J. Simple Connections. Publ.126 ed. Brussels: ECCS Press; 2009.
22. Castro JM, Elghazouli AY, Izzudin BA. Modelling of the panel zone in steel and composite moment frames. Engineering Structures. 2005;27:129-144.
23. Bravo M, Herrera R. Performance under cyclic load of built-up T-stubs for Double T moment connections. Journal of Constructional Steel Research. 2014;103:117-130.
24. Dubina D, Montreau N, Stratau A, Grecea D, Zaharia R. Testing program to evaluate behavior of dual steel connections under monotonic and cyclic loading. Paper presented at: Proceedings of the 5th European Conference on Steel and Composite Structures, 2008; Graz, Austria.
25. Kim KD, Engelhardt MD. Monotonic and cyclic loading models for panel zones in steel moment frames. Journal of Cosntructional Steel Research. 2002;58:605-635.

26. Saberi V, Gerami M, Kheyroddin A. Comparison of bolted end plate and T-stub connection sensitivity to component thickness. Journal of Constructional Steel Research. 2014;98:134-145.
27. Nogueiro P, Simoes da Silva L, Bento R, Simoes R. Calibration of Model Parameters for the Cyclic Response of End-Plate Beam-to-Column Steel-Concrete Composite Joints. Journal of Steel and Composites Structures. 2009;9(1):35-58.
28. Kim Y, Ryu H, Kang C. Hysteretic Behaviour of Moment Connections with Energy Absorption Elements at Beam Bottom Flanges. Paper presented at: ICAS 2007, 2007; Oxford.
29. Latour M, Rizzano G. Experimental Behavior and Mechanical Modeling of Dissipative T-Stub Connections. Journal of Structural Engineering. 2012;138(2):170-182.
30. Latour M, Rizzano G. Design of X-shaped double split tee joints accounting for moment-shear interaction. Journal of Constructional Steel Research. 2015c;104:115-126.
31. Inoue K, Suita K, Takeuchi I, Chusilp P, Nakashima M, Zhou F. Seismic-Resistant Weld-Free Steel Frame Buildings with Mechanical Joints and Hysteretic Dampers. Journal of the Structural Engineering, ASCE. 2006;132(6):864-872.
32. Kishiki S, Yamada S, Suzuki K, Saeki E, Wada A. New Ductile Moment-Resisting Connections Limiting Damage to Specific Elements at the Bottom Flange., 2006; San Francisco.
33. Christopoulos C, Filiatrault A. Principles of Passive Supplemental Damping and Seismic Isolation. Pavia: IUSS PRESS; 2006.
34. Soong TT, Spencer Jr BF. Supplemental Energy Dissipation: State-of-the-Art and State-of-the-Practice. Engineering Structures. 2002;24:243-259.
35. Mualla I, Belev B. Seismic Response of Steel Frames Equiped with a New Friction Damper Device Under Earthquake Excitation. Engineering Structures. 2002;24(3):365-371.
36. Oh S, Kim Y, Ryu H. Seismic Performance of Steel Structures with slit dampers. Engineering Structures. 2009;31:1997-2008.

37. Latour M, Piluso V, Rizzano G. Experimental behaviour of friction T-stub beam-to-column joints under cyclic loads. Steel Construction (1). 2013b.
38. Yan T, Popov E. Experimental and analytical studies of steel connections and energy dissipators. Berkeley: Earthquake Engineering Research Center; 1995. UCB/EERC-95/13.
39. Khoo H, Clifton G, Macrae G, Ramhormozian S. Proposed design models for the asymmetric friction connection. EARTHQUAKE ENGINEERING & STRUCTURAL DYNAMICS. December 2014;44(8):1309-1324.
40. Khoo H, Clifton C, Butterworth J, MacRae G, Gledhill S, Sidwell G. Development of the self-centering Sliding Hinge Joint with friction ring springs. Journal of Constructional Steel Research. 2012a;78:201-211.
41. Khoo H, Clifton J, Butterworth J, Macrae G. Experimental Study of Full-ScaleSelf-Centering Sliding Hinge JointConnections with Friction Ring Springs. Journal of Earthquake Engineering. September 2013(17):972-997.
42. Borzouie J, Macrae G, Chase J, et al. Cyclic Performance of Asymmetric Friction Connections with Grade 10.9 Bolts. The Bridge and Structural Engineer. March 2015;45(1).
43. Latour M, Piluso V, Rizzano G. Experimental analysis of innovative dissipative bolted double split tee beam-to-column connections. Steel Construction. June 2011a;4(2):53-64.
44. Yeung S., Zhou H., Khoo H.H., Clifton G.C., MacRae G.A. Sliding shear capacities of the Asymmetric Friction Connection. 2013 NZSEE Conference, April 26-28, Wellington, 2013. Paper n. 27,
45. Butterworth J.W., Clifton G.C., Performance of Hierarchical Friction Dissipating Joints in Moment Resisting Steel Frames. 12 World Conference on Earthquake Engineering, Paper N. 718, 2000.
46. Latour M, Piluso V, Rizzano G. Experimental Analysis of Friction Materials for supplemental damping devices. Construction and Building Materials. 2014b.
47. Latour M, Piluso V, Rizzano G. Free from damage beam-to-column joints: Testing and design of DST connections with friction pads. Engineering Structures. 2015a;85:219-233.

48. Ono S, Nakahira K, Tsujioka S, Uno N. Energy Absorption Capacity of Thermally Sprayed Aluminum Friction Dampers. Journal of Thermal Spray Technology. September 1996;5(3).
49. Sato A, Kimura K, Suita K, Inoue K. Cyclic Test of High Strength Steel Beam-to-Column Connection Composed with Knee-Brace Damper and Friction Damper Connected by High Strength Bolts, 2009; Proceedings of the SEEBUS 2009. Kyoto, Japan.
50. D'Aniello M., Cassiano D., Landolfo R., (2016) Monotonic and cyclic inelastic tensile response of European preloadable GR10.9 bolt assemblies. Journal of Constructional Steel Research, 124: 77–90.
51. D'Aniello M., Cassiano D., Landolfo R., (2017) Simplified criteria for finite element modelling of European preloadable bolts. Steel and Composite Structures, An International Journal Vol. 24, No. 6 (2017) 643-658
52. Heistermann C. Behaviour of Pretensioned Bolts in Friction Connections. Lulea: Lulea University of Technology; 2011.
53. Schnorr. Handbook for Disc Springs. Heilbronn: Adolf Schnorr GmbH; 2003.
54. UNI-CEI-CNR. Costruzioni di acciaio. Istruzioni per il calcolo, l' esecuzione, il collaudo e la manutenzione. Steel structures. Instructions of design, construction, testing and maintenance.: UNI; 1988.
55. CEN. UNI EN 1090-2. Steel structures. Instructions of design, construction, testing and maintenance.Steel structures. Instructions of design, construction, testing and maintenance.; 2008.
56. Paciello A. Progettazione e analisi delle prestazioni sismiche di sistemi accoppiati in acciaio con collegamenti di tipo "FREEDAM". MSc - Università degli Studi di Salerno: Tesi di laurea in Ingegneria edile-architettura; 2015.
57. Heistermann C, Veljkovic M, Simoes R, Rebelo C, Simoes da Silva L. Design of slip resistant lap joints with long open slotted holes. Journal of Constructional Steel Research. 2012;82:223-233.
58. Kulak G, Fisher J, Struik J. Guide to design criteria for bolted and riveted joints: Research Council on Structural Connections; 2001.
59. AISC. Seismic Provisions for Structural Steel Buildings. Chicago, Illinois; 2005.

60. Golondrino JC, MacRae G, Chase J, Rodgers G., Clifton GC. Velocity effects on the behavior of asymmetrical friction connections (AFC). 8th STESSA Conference, Shanghai, China, July 1-3, 2015
61. Ferrante Cavallaro, G., Latour, M., Francavilla, A.B., Piluso, V., Rizzano, G. Standardised friction damper bolt assemblies time-related relaxation and installed tension variability (2018) Journal of Constructional Steel Research, 141, pp. 145-155.